ÇUKUROVA UNIVERSITY
INSTITUTE OF NATURAL AND APPLIED SCIENCES

MSc THESIS

Alişah NART

DETERMINATION OF UNDERLYING EVENT CONTRIBUTION TO THE JET ENERGIES IN CMS HEAVY ION COLLISIONS

DEPARTMENT OF PHYSICS

ADANA, 2011

ÇUKUROVA UNIVERSITY
INSTITUTE OF NATURAL AND APPLIED SCIENCES

DETERMINATION OF UNDERLYING EVENT CONTRIBUTION TO THE JET ENERGIES IN CMS HEAVY ION COLLISIONS

Alişah NART

MSc THESIS

DEPARTMENT OF PHYSICS

We certify that the thesis titled above was reviewed and approved for the award of degree of the Master of Science by the board of jury on 16/12/2011.

…………………………….	……………………….	………………………………….
Prof. Dr. İsa DUMANOĞLU	Prof. Dr. Sefa ERTÜRK	Prof. Dr. Aysel KAYIŞ TOPAKSU
SUPERVISOR	MEMBER	MEMBER

This MSc Thesis is written at the Department of Institute of Natural And Applied Sciences of Çukurova University.
Registration Number:

Prof. Dr. İlhami YEĞİNGİL
Director
Institute of Natural and Applied Sciences

ABSTRACT

MSc THESIS

DETERMINATION OF UNDERLYING EVENT CONTRIBUTION TO THE JET ENERGIES IN CMS HEAVY ION COLLISIONS

Alişah NART

ÇUKUROVA UNIVERSITY
INSTITUTE OF NATURAL AND APPLIED SCIENCES
DEPARTMENT OF PHYSICS

Supervisor :Prof. Dr. İsa DUMANOĞLU
Year: 2011, Pages: 43
Jury :Prof. Dr. İsa DUMANOĞLU
:Prof. Dr. Sefa ERTÜRK
:Prof. Dr. Aysel KAYIŞ TOPAKSU

The aim of nucleus-nucleus collisions at the ultra relativistic colliders is obtaining the hot and dense partonic matter. This partonic matter is required to study fundamental of quantum chromo dynamics (QCD). This hot and dense matter is reach the extremely high temperature and energies at the nuclei collisions. At the first moments of the nuclei collisions, the temperature of Quark gluon plasma and its density went down when the plasma going in to stable and during the this dense and temperature change is open the way of hadronization process for the QGP. There is two way to observe the properties of QGP, soft probes and hard probes. This thesis focused on the one of the hard probes; jets. The energy of jets, reconstruction of jet and background contribution to jet energy is studied and investigated well.

Key Words: Heavy Ion, CMS, Background Subtraction, Efficiency of Pile Subtraction Algorithm, Iterative Cone Jet Algorithm

ÖZ

MASTER TEZİ

CMS AĞIR İYON ÇARPIŞMALARINDA ARKA PLAN OLAYLARININ JET ENERJİLERİNE KATKISININ BELİRLENMESİ

Alişah NART

ÇUKUROVA ÜNİVERSİTESİ
FEN BİLİMLERİ ENSTİTÜSÜ
FİZİK ANABİLİM DALI

Danışman :Prof. İsa DUMANOĞLU
Yıl: 2011, Sayfa: 43
Jüri :Prof. İsa DUMANOĞLU
:Prof. Dr. Sefa ERTÜRK
:Prof. Dr. Aysel KAYIŞ TOPAKSU

Yüksek enerjili hızlandırıcılarda ağır iyon fiziği çalışılmasının amacı yüksek sıcaklık ve yoğunlukta partonik bir madde elde edebilmektir. Bu partonik madde kuantum renk dinamiği çalışmaları için gereklidir. Bu yoğun ve sıcak maddeye çekirdek-çekirdek etkileşmelerinde ulaşılabilir. Çekirdek çarpışmalarının ilk aşamalarından denge durumuna geçerken kuark gluon plazmasının sıcaklığı ve yoğunluğu azalmaya başlar ve bu esnada hadranizasyona geçişi söz konusudur. Kuark gluon plazması durumunun araştırılması ve özelliklerinin belirlenmesi için iki tip sonda kullanılır. Bunlar sert sonda ve yumuşak sonda olmak üzere iki ana başlıkta toplanır. Bu tez sert sondalardan biri olan jetler üzerine odaklanmıştır. Jetlerin enerjisi, yapılandırılması ve jet enerjisine ardalan katkısı incelenmiştir.

Anahtar Kelimeler: Ağır İyon, CMS, Fon Çıkarımı, Üst Üste Binme Algoritmasının Verimliliği, Tekrarlayan Koni Jet Algoritması

ACKNOWLEDGEMENT

I would like to thank my supervisor Prof. İsa Dumanoğlu for his precious guidance, encouragement and support during my MSc degrees.

I would like to thank my friend and colleague Yetkin Yılmaz for his support during my analysis.It was a pleasure for me to work with him. Also I would like to thank members of the Heavy Ion Group at CMS. The weekly-daily meetings theyhad gave me a chance to learn a lot from them, especially Christoph Roland, Frank Ma, Gunther Roland, Bolek Wyslouch and other Heavy Ion Group participants.

Special thanks are due to my dear friend Nazlı Bahar Özkan for sharing her optimistic attitude and encouragement even at my hard times and valuable comments, suggestions and support during writing of this thesis.

CONTENTS **PAGE**

LIST OF TABLES **PAGE**

LIST OF FIGURES **PAGE**

ABBREVATIONS

ALICE	: A Large Ion Collider Experiment
ATLAS	: A Toroidal LHC ApparatuS
CERN	: Conceil Europeenne pour la Recherche Nucleaire
CMS	: Compact Muon Solenoid
ECAL	: Electromagnetic Calorimeter
EM	: Electro Magnetic
GeV	: Giga Electron Volt
HAD	: Hadronic
HB	: Hadronic Barrel
HCAL	: Hadronic Calorimeter
HE	: Hadronic Endcap
HO	: Hadronic Outer
HF	: Hadronic Forward
L	: Luminosity
LEP	: Large Electron Positron Collider
LHC	: Large Hadron Collider
LHC-b	: Large Hadron Collider Beauty Experiment
MET	: Missing Transverse Energy
MC	: Monte Carlo
PS	: Proton Synchrotron
QCD	: Quantum Chromo Dynamics
QGP	: Quark-Gluon-Plasma
RHIC	: Relativistic Heavy Ion Collider
SPS	: Super Proton Synchrotron
SM	: Standart Model
TeV	:Trillion Electron Volt
$\sqrt{s}$	: Center of Mass Energy

1. INTRODUCTION

The Standard Model (SM) has been developed by particle physicists to describe what the Universe is made of. It is an elemental and comprehensive theory that explains all the properties of matter and their complex interactions. There are 6 quarks and 6 leptons and also there are 6 antiquarks and 6 antileptons. The interactions are mediated by force carrier particles, like photon, W^{+}, W^{-}, Z^{0} bosons and gluons. The matter particles, which are grouped into three generations according to their masses, and the basic force carrier particles (bosons) are shown in Table 1.1.

Table 1.1. Standard Model of Elementary Particles.

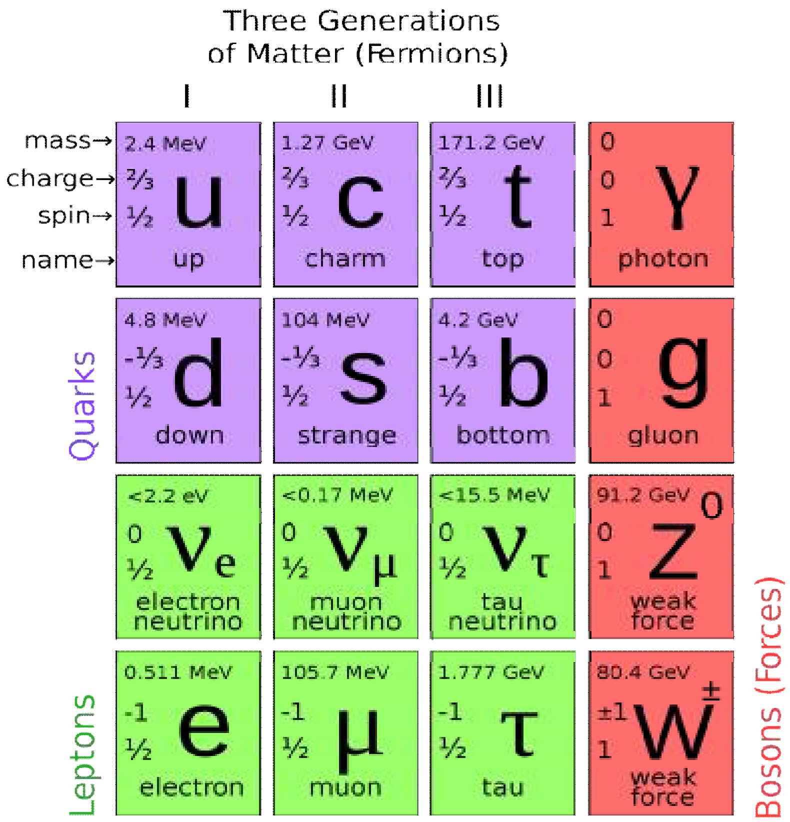

Experiments have verified SM predictions to incredible precision, and all the particles predicted by this theory have been found except the Higgs boson, which is included in the theory to explain the different masses of the particles. However, it does not explain everything. For example, gravity is not included in the SM. For each kind of matter particle there is a corresponding antimatter particle or antiparticle. If antimatter and matter are exactly equal but have opposite charge, then why there is so much matter in the universe than antimatter?

The Large Hadron Collider (LHC) project at the European Organization for Nuclear Research (CERN), near Geneva in Switzerland, is designed to find answers to these questions.

High-energy collisions of heavy ions allow to study the fundamental theory of the strong interaction — Quantum Chromo Dynamics (QCD) — under extreme temperature and density conditions. A new form of matter formed at the energy densities above ≈1 GeV/fm^3 is predicted in Lattice QCD calculations. This quark-gluon plasma (QGP) consists of an extended volume of deconfined and chirally symmetric quarks and gluons.

Heavy ion collisions at the Large Hadron Collider (LHC) are expected to produce matter at energy densities exceeding any previously explored in experiments conducted at particle accelerators. Preliminary results for fully reconstructed jets at RHIC, measured in Au-Au collisions at $\sqrt{s_{NN}}$ =200 GeV (STAR Collaboration, 2009), and there was also hints of broadened jet shapes due to medium-induced gluon radiation.

The jet analysis presented in this thesis was performed using the data collected in 2010 from Pb-Pb collisions at a nucleon-nucleon center-of-mass energy of $\sqrt{s_{NN}}$ = 2.76 TeV at the Compact Muon Solenoid (CMS) detector. The CMS detector has a solid angle acceptance of nearly 4π and is designed to measure jets and energy flow, which are ideal feature for studying heavy ion collisions.

A total integrated (Pb-Pb) luminosity of 7.96 μb^{-1} was collected. Jets were reconstructed based on their energy deposits in the CMS calorimeters.

2. MATERIAL AND METHOD

2.1. Large Hadron Collider (LHC)

The LHC is presently being constructed in the already existing 27-km LEP tunnel. The LHC is designed to collide head-on two opposite rotating beams of protons or heavy ions. Proton-proton collisions are planned at a centre-of-mass energy of $\sqrt{s_{NN}}$ =14 TeV which is 7 times higher than the*p-p* collisions of Tevatron, Fermilab. Moreover, the LHC will supply heavy ion (lead) collisions with a centre-of-mass energy per nucleon $\sqrt{s_{NN}}$ =2.76 TeV. This energy level is about30 times higher than the Relativistic Heavy Ion Collider (RHIC) at the Brookhaven Laboratory (CMS TDR, 2007).

The prime motivation of the LHC is to elucidate the nature of electroweak symmetry breaking for which the Higgs mechanism is presumed to be responsible. The experimental study of the Higgs mechanism can also shed light on the mathematical consistency of the Standard Model at energy scales above about 1 TeV. Various alternatives to the Standard Model invoke new symmetries, new forces or constituents. Furthermore, there are high hopes for new discoveries that could pave the way toward a unified theory. These discoveries could take the form of supersymmetry or extra dimensions, the latter often-requiring modification of gravity at the TeV scale. Hence there are many compelling reasons to investigate the TeV energy scale.

The LHC will provide high-energy heavy-ion collisions which allowing us to further extend the study of QCD matter under extreme conditions of temperature, density, and parton momentum fraction (low-*x*).

Hadron colliders are well suited to the task of exploring new energy domains, and the region of 1 TeV constituent centerofmass energy can be explored if the ion energy and the luminosity are high enough. The beam energy and the design luminosity of the LHC have been chosen in order to study physics at the TeV energy scale. A wide range of physics is potentially possible with the seven-fold increase in energy and a hundred-fold increase in integrated luminosity over the previous hadron collider experiments. These conditions also require a very careful design of the detectors.

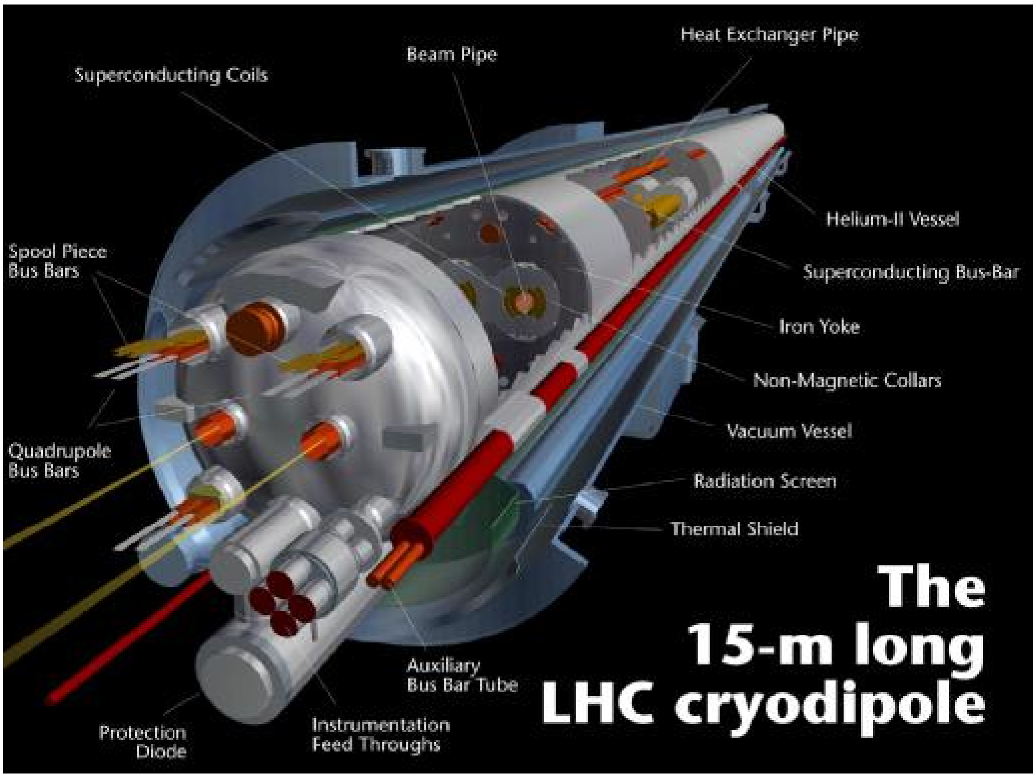

Figure 2.1. The Part of LHC machine - the 1232 dipoles bend the beam around the 27 km circumference.

2.2. Compact Muon Solenoid(CMS)

The main distinguishing features of CMS are a high-field solenoid, a full-silicon-based inner tracking system, and a homogeneous scintillating-crystals-based electromagnetic calorimeter. The coordinate system adopted by CMS has the origin centered at the nominal collision point inside the experiment, the *y*-axis pointing vertically upward, and the *x*-axis pointing radially inward toward the center of the LHC. Thus, the *z*-axis points along the beam direction toward the Jura Mountains from LHC Point 5. The azimuthal angle ϕ is measured from the *x*-axis in the *x*-*y* plane and the radial coordinate in this plane is denoted by *r*. The polar angle θ is measured from the z-axis. Pseudorapidity is defined as $\eta = -\ln\tan(\theta/2)$. Thus, the momentum and energy transverse to the beam direction, denoted by $p_T$and E_T, respectively, are computed from the x and y components. The imbalance of energy measured in the transverse plane is denoted by E_T^{miss}.

The overall layout of CMS is shown in Figure 2.2. At the heart of CMS a 13-m long, 6-m-inner-diameter, 4-T superconducting solenoid sits to provide large bending power (12 Tm) before the muon bending angle is measured by the muon system. The return field is large enough to saturate 1.5 m of iron, allowing 4 muon stations to be integrated to ensure robustness and full geometric coverage. Each muon station consists of several layers of aluminium drift tubes (DT) in the barrel region and cathode strip chambers (CSC) in the endcap region, complemented by resistive plate chambers (RPC). The bore of the magnet coil is large enough to accommodate the inner tracker and the calorimeter inside. A cylinder of 5.8-m length and 2.6-m diameter gives the tracking volume.

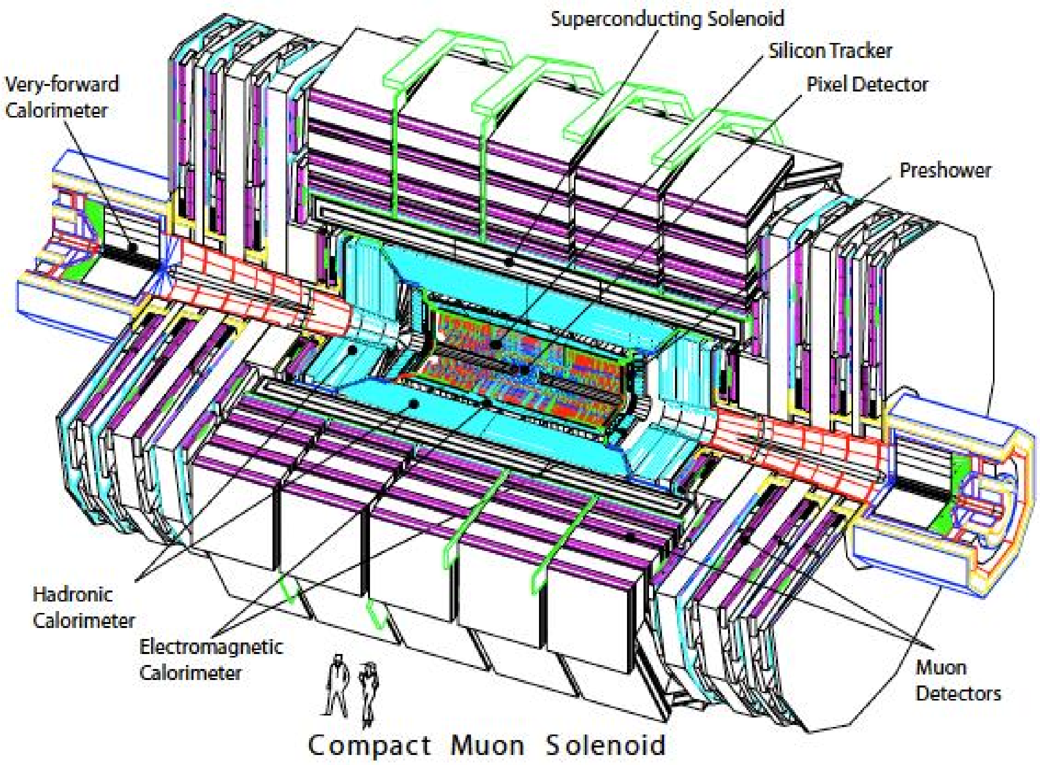

Figure 2.2. The CMS Detector.

In order to deal with high track multiplicities, CMS employs 10 layers of silicon micro strip detectors, which provide the required granularity and precision. In addition, 3 layers of silicon pixel detectors are placed close to the interaction point to improve the measurement of the impact parameter of charged-particle tracks, as well as the position of secondary vertices.

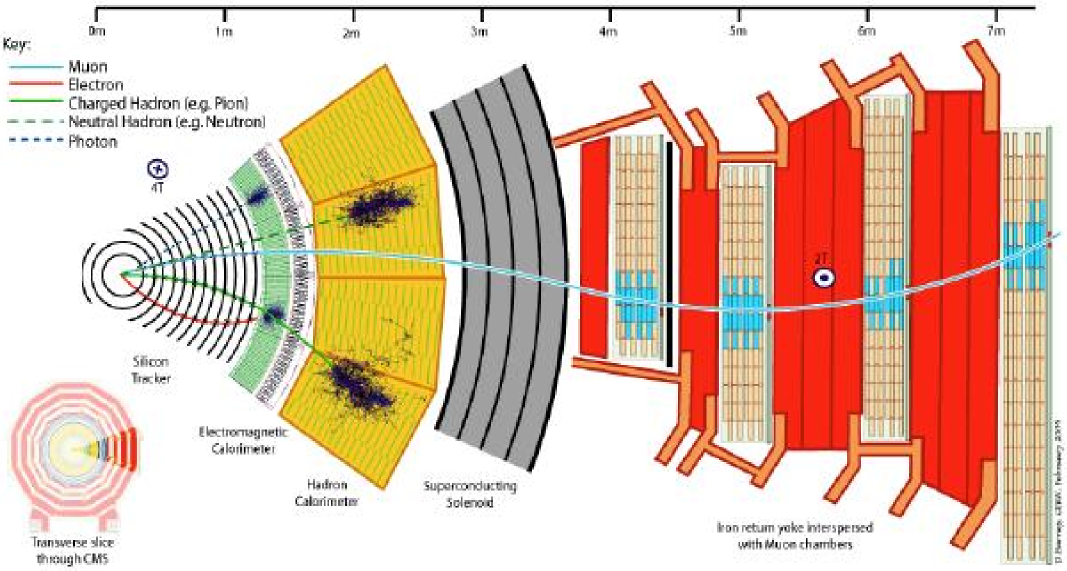

Figure 2.3. A transverse slice through one segment of the CMS detector indicating the responses of the various detecting systems to different types of particles.

The responses of CMS subdetectors to different types of particles shown in Figure 2.3.The electromagnetic calorimeter (ECAL) uses lead tungstate ($PbWO_4$) crystals with coverage in pseudorapidity up to $|\eta| < 3.0$. The scintillation light is detected by silicon avalanche photodiodes (APDs) in the barrel region and vacuum phototriodes (VPTs) in the endcap region. A preshower system is installed in front of the endcap ECAL for π^0 rejection. The ECAL is surrounded by a brass/scintillator sampling hadron calorimeter (HCAL) with coverageup to $|\eta| < 3.0$. The scintillation light is converted by wavelength-shifting (WLS) fibersembedded in the scintillator tiles and channeled to photodetectors via clear fibers. This light isdetected by photodetectors (hybrid photodiodes, or HPDs) that can provide gain and operate inhigh axial magnetic fields. This central calorimeter is complemented by a tailcatcher in the barrelregion (HO) ensuring that hadronic showers are sampled with nearly 11 hadronic interactionlengths. Coverage up to a pseudorapidity of 5.0 is provided by an iron/quartz-fibre calorimeter.The Cherenkov light emitted in the quartz fibers is detected by photomultipliers. The forwardcalorimeters ensure full geometric coverage for the measurement of the transverse energy in theevent. An even higher forward coverage is obtained with additional dedicated calorimeters and with the TOTEM tracking detectors.

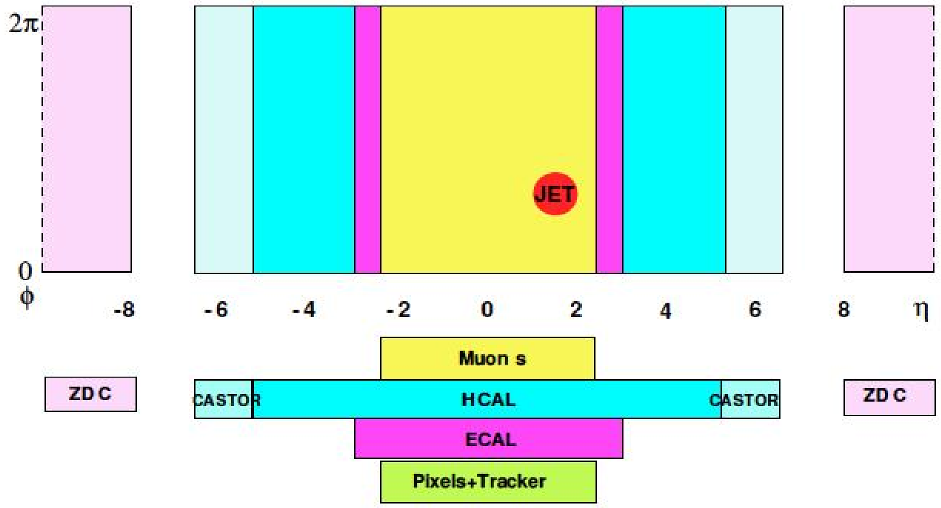

Figure 2.4. CMS acceptance of tracking, calorimeter, and muon identification in pseudorapidity (η) and azimuth (ϕ). The size of a jet with cone R = 0.5 is also depicted for illustration

Acceptance of CMS tracking, calorimeter and muon systems in η and ϕ coordinates shown in Figure 2.4. The detector requirements for CMS to meet the goals of the LHC physics programme can be summarized as follows:

• Good muon identification and momentum resolution over a wide range of momenta and angles, good dimuon mass resolution (≈ 1% at 100 GeV), and the ability to determine unambiguously the charge of muons with p< 1 TeV;

• Good charged particle momentum resolution and reconstruction efficiency in the inner tracker. Efficient triggering and offline tagging of τ's and b-jets, requiring pixel detectors close to the interaction region;

• Good electromagnetic energy resolution, good diphoton and dielectron mass resolution (≈ 1% at 100 GeV), wide geometric coverage, π^0 rejection, and efficient photon and lepton isolation at high luminosities;

• Good missing-transverse-energy and dijet-mass resolution, requiring hadron calorimeters with a large hermetic geometric coverage and with fine lateral segmentation.

2.3.Heavy Ion Observables in CMS

2.3.1.High-Energy Nucleus-Nucleus Collisions

The study of the fundamental theory of the strong interaction — Quantum Chromodynamics (QCD) — in extreme conditions of temperature, density and parton momentum fraction (low-*x*) has attracted an increasing experimental and theoretical interest during the last 20 years. Indeed, QCD is not only a quantum field theory with an extremely rich dynamical content — such as asymptotic freedom, infrared slavery, (approximate) chiral symmetry, non-trivial vacuum topology, strong CP violation problem, UA(1) axial-vector anomaly, colour superconductivity, etc. — but also the only sector of the Standard Model (SM) whose full *collective* behaviour — phase diagram, phase transitions, thermalisation of fundamental fields — is accessible to scrutiny in the laboratory. The study of the many-body dynamics of high-density QCD covers a vast range of fundamental physics problems (see the Figure 2.5.).

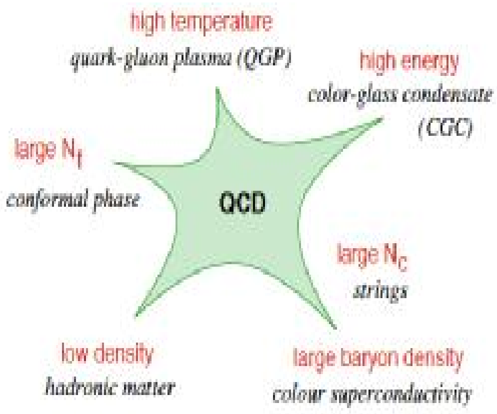

Figure 2.5. Many-body dynamics of QCD in different physics limits.

The only experimental means available so far to investigate the thermodynamics of a multiparton system involves colliding large atomic nuclei at ultra relativistic energies. Figure 2.6, shows the total centre-of-mass energy available for particle production (i.e. subtracting the rest mass of the colliding hadrons) at different accelerators as a function of the first operation year ("Livingston plot") (Schukraft, 2006). The exponential increase in performance translates into an energy doubling every 2 (3) years for the ion (*pp*) beams(CMS TDR, 2007).

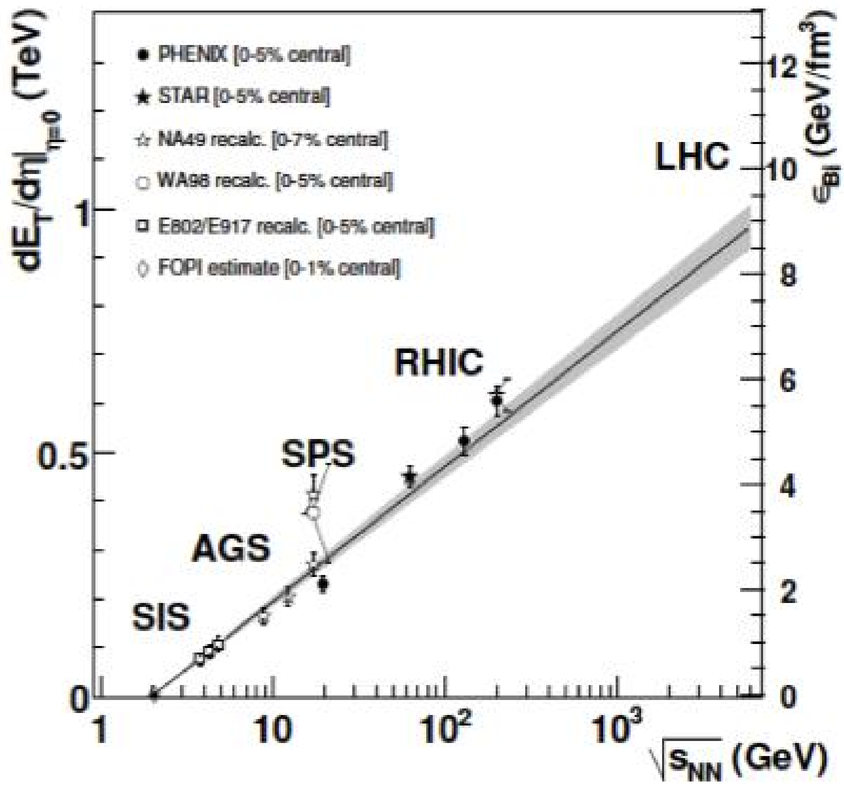

Figure 2.6. "Livingston plot" for proton and ion accelerators in the period 1960-2008.

Head-on collisions of heavy ions can produce extremely hot and dense QCD matter by concentrating a substantial amount of energy — O(1 TeV) at mid-rapidity at the LHC, see Figure 2.7 — in an *extended* cylindrical volume, $V = \pi R^2 A \tau_0 150$ fm^3 for a typical large nucleus with radius R_A= 6.5 fm, at thermalisation times of τ_0= 1 fm/c (CMS TDR, 2007).

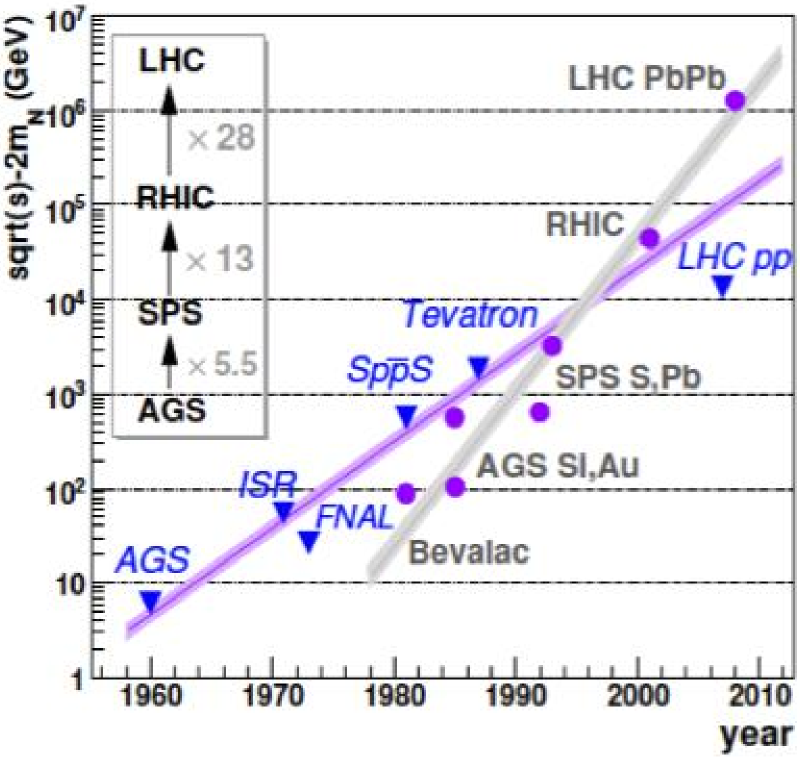

Figure 2.7.Measured transverse energy per unit rapidity atη = 0 and corresponding Bjorken energy density, in central heavy-ion collisions at various center of mass energies, fitted to a logarithmic parametrisation

2.3.2. Hard Probes at Heavy Ion Physics: Jet Physics

Before giving the definition of a jet, notice that for large-momentum-transfer processes, as becomes small, and analytic calculations through perturbation theory become possible. In this context, we can understand why these so-called ***hard processes*** played such an important role in the first tests of QCD.

In particular, the experimental study of these hard processes was performed through the study of the properties of the final state particles produced in the collisions of simple QCD systems such as e^+e^-,two protons or a proton and an antiproton (Owens, 1987). In the spirit of confinement and the running coupling constant, we can understand some qualitative features of these final state particles as follows. When a large-momentum transfer occurs in a high-energy collision in such a simple system, as the original scattered partons separate, the energy in the strong field between them becomes bigger and bigger until there is enough energy to create a new quark-antiquark pair. This process results in the production of a set of particles travelling in random directions and concentrated in small cones around the direction of the original partons after the scattering process. These set of particles were called *QCD jets.*

Summarizing, a QCD jet is the highly collimated set of hadronic particles generated by a high-momentum-transfer scattering due to strong interactions at the partonic level. While this definition is simple and gives insight into the nature of a jet, it is experimentally rather simplistic and not suitable.

In principle, extrapolating the description of a hard process given above and in the absence of a phase transition and the resulting collective phenomena, we would expect many such jets to appear in more complex systems such as those encountered in heavy-ion collisions. The absence of such a superposition in fact has been pointed as one of the signatures of the existence of the QGP. However, even if the QGP is formed over the region of space where the heavy-ion collision occurs, we do expect to have a certain number of hard scatterings whose final state radiation is not completely dominated by the collective phenomena resulting from the QGP formation. Note that wherever one such scattering occurs, it will have at least one initial parton scattered into the QGP. The modification that the jet coming from this parton suffers due to the interaction of the parton with the QGP is what we refer to as Jet Quenching. Jet quenching has already been observed at RHIC (Star Collaboration, 2009). However, the new energy scale accessible at the LHC and the design of the detectors operating there, will allow to study the jet quenching phenomenon in more depth, allowing us to learn about the properties of the QGP and the interactions within it (Wiedemann*et al, 2003*).

Jet quenching is one of the promising tools, which is available at the LHC in order to study the properties of the QGP. However, the theoretical definition of a jet is not explicit enough to be useful even at the most basic Monte Carlo level. In particular, we need to define the level of collimation of a set of particles to be considered a jet. The parameterization of such level of collimation is done differently in different jet-finding algorithms. For first CMS HI collisions, the Iterative Cone algorithmwas used becauseof its simpleimplementation and providing good resolution if compared to the fluctuations introduced by the subtraction of the background. In iterative cone algorithms, a jet is defined as a cone of particles in η x $f$space. The radius of this cone then gives the degree of collimation. Typical values of this radius are in the 0.3 to 0.7 ranges. While a large radius might be impractical for jet reconstruction in the presence of a heavy-ion background, using a too small radius may miss essential features of the jet quenching mechanism, which may de-collimate the jet. CMS HI group, therefore, decided to use a cone of radius 0.5 which reconstructs almost 90% of the energy in the jet and is also usable with our algorithm for background subtraction.

Another parameter, which enters our experimental definition of a jet, is the jet energy, E or E_{T} the sum of the transverse energies of the particles inside the jet cone. We used the Iterative Cone algorithm to find such objects. The idea behind this algorithm is to initially consider as jet candidates the cones around the most energetic particles, and then modify the axis of the candidate jet to account for the energy distribution inside the candidate jet cone. This procedure, which is systematically outlined in Section 2.3.6, is iterated until the jet axis is not being modified much or a maximum number of iterations is exceeded.

2.3.3. Data Samples And Triggers

The measured cross section for hadronic inelastic PbPbcollisions at $\sqrt{s_{NN}}$ = 2.76 TeV is ~7.96 μb^{-1}. In addition, there is a sizable contribution from large impact parameter ultra-peripheral collisions (UPC) that lead to the electromagnetic breakup of one, or both, of the Pb nuclei (CMS Collaboration, 2010). Particles per unit of pseudorapidity, depends on the impact parameter.

For online event selection, CMS uses a two-level trigger system: Level-1 (L1) and High Level Trigger (HLT). The events for CMS HI collisions, were selected using an inclusive single-jet trigger that required an L1 jet with p_{T}> 30 GeV/c and an HLT jet with p_{T}> 35GeV/c, p_{T}wasn't corrected for the $p_T$dependencyof the calorimeter energy response. The efficiency of the jet trigger is shown in Figure 2.8 for leading jets with $|\eta|$ < 2 as a function of their corrected p_{T}. The efficiency is defined as the ratio of the number of triggered events over the number of minimum bias events. The trigger becomes fully efficient for collisions with a leading jet with corrected p_T greater than 100 GeV/c.

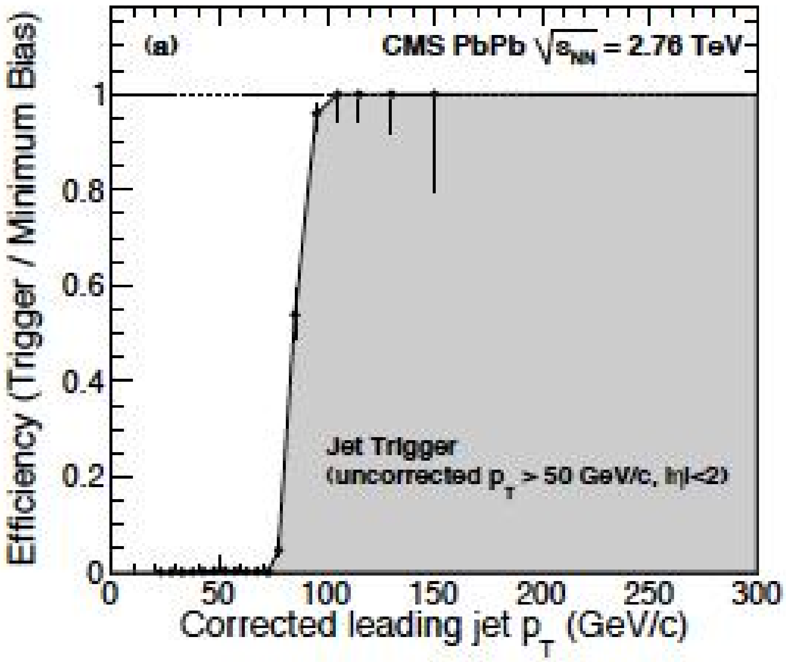

Figure 2.8.Efficiency curve for the HLT 50 GeV/c single-jet trigger, as a function of the corrected leading jet transverse momentum.

In addition to the jet data sample, a minimum bias event sample was collected using coincidences between the trigger signals from the +*z* and −*z* sides of either the BSC or the HF. This trigger has efficiency more than 97% for hadronic inelastic collisions.

In order to suppress non-collision related noise, cosmic rays, double-firing triggers, and beam backgrounds, the minimum bias and jet triggers used in this analysis were required to fire in time with the presence of both colliding ion bunches in the interaction region. It was checked that the events selected by the jet trigger described above also satisfy all triggers and selections imposed for minimum bias events. The total hadronic collision rate varied between 1 and 210 Hz, depending on the number of colliding bunches (between 1×1 and 129×129) and on the bunch intensity (CMS Collaboration, 2010).

2.3.4. Event Selection

In order to select a pure sample of inelastic hadronic collisions for analysis, a number of offline selections were applied to the triggered event samples, removing contaminations from UPC events and non-collision beam backgrounds (e.g. beam-gas). Table 2.1 shows the number of events remaining after the various selection criteria are applied. First, beam halo events were vetoed based on the timing of the $+z$ and $-z$ BSC signals. Then, to veto UPC and beam-gas events, an offline HF coincidence of at least three towers on each side of the interaction point was required, with a total deposited energy of at least 3 GeV. Next, a reconstructed vertex was required with at least two tracks of $p_T > 75$ MeV/c, consistent with the transverse beam spot position and the expected collision region along the z-axis. Finally, to further reject beam-gas and beam-scraping events, the lengths of pixel clusters along the beam direction were required to be compatible with particles originating from the primary vertex.

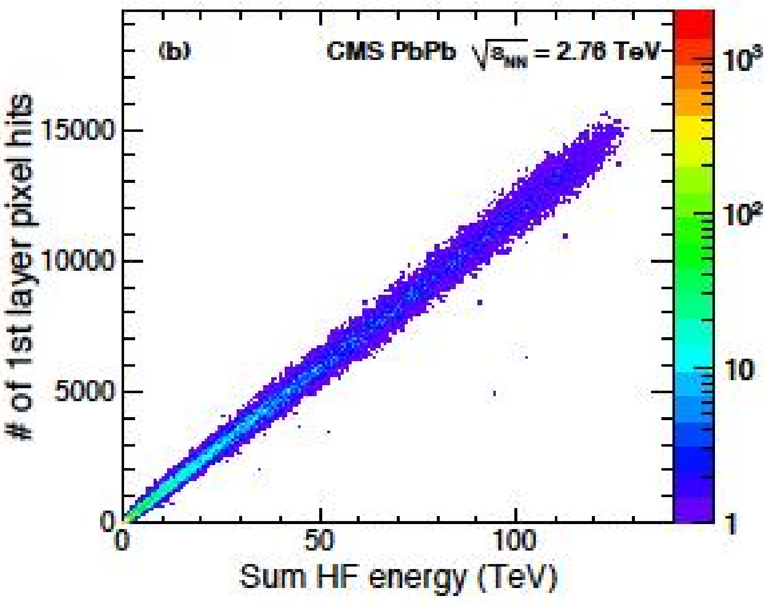

Figure 2.9. Correlation between the number of pixel hits and HF total energy, after selections as described in the text.

Figure 2.9 shows the correlation between the total energy deposited in the HF calorimeters and the number of hits in the first layer of the silicon pixel barrel detector after these event selections. A tight correlation between the two detectors is observed, with very few events showing HF energy deposits that deviate significantly (at any given number of pixel hits) from the expectations for hadronicPb-Pb collisions. This correlation is important to verify the selection of a pure collision event sample, and also to validate the HF energy sum as a measure of event centrality. Prior to jet finding on the selected events, a small contamination of noise events from uncharacteristic ECAL and HCAL detector responses was removed using signal timing, energy distribution, and pulse-shape information. As a result, about 2% of the events were removed from the sample (CMS Note, 2010).

Table 2.1. Event selection criteria used for this analysis. The percentages of events remaining after each criterion, listed in the last column, are with respect to the previous criterion (the event selection criteria are applied in the indicated sequence).

Criterion	Events remaining	% of events remaining
Jet triggered events ($p_T^{uncorr} > 50$ GeV/c)	149 k	100.00
No beam halo, based on the BSC	148 k	99.61
HF offline coincidence	111 k	74.98
Reconstructed vertex	110 k	98.97
Beam-gas removal	110 k	99.78
ECAL cleaning	107 k	97.66
HCAL cleaning	107 k	99.97
≥ 2 jets with $p_T > 35$ GeV/c and $\lvert\eta\rvert < 2$	71.9k	67.07
Leading jet $p_{T,1} > 120$ GeV/c	4 216	5.86
Subleading jet $p_{T,2} > 50$ GeV/c	3 684	87.38
$\Delta\phi_{12}$ of 2 jets $> 2\pi/3$	3 514	95.39

2.3.5. Centrality Determination

For the analysis of *Pb-Pb* events, it is important to know the “centrality” of the collision, i.e., whether the overlap of the two colliding nuclei is large or small. In first heavy ion collisions at LHC, the observable used to determine centrality is the total energy from both HF calorimeters. The distribution of theenergy of HF calorimeter is shown in Figure 2.10. The shape of the energy distribution is characteristic of all observables related to particle production in heavy ion collisions. The more frequent peripheral events with large impact parameter produce very few particles, while the central events with small impact parameter produce many more particles because of the increased number of nucleon-nucleon interactions.

The distribution of HF total energy was used to divide the event sample into 40 centrality bins, each representing 2.5% of the total nucleus-nucleus interaction cross section. Because of inefficiencies in the minimum bias trigger and event selection, the obtained multiplicity distribution does not represent the full interaction cross section. MC simulations were used to presume the distribution in the regions where events are lost. Comparing the simulated distribution to the obtained distribution, it is estimated that the minimum bias trigger and event selection efficiency is about97±3%(CMS Note, 2010).

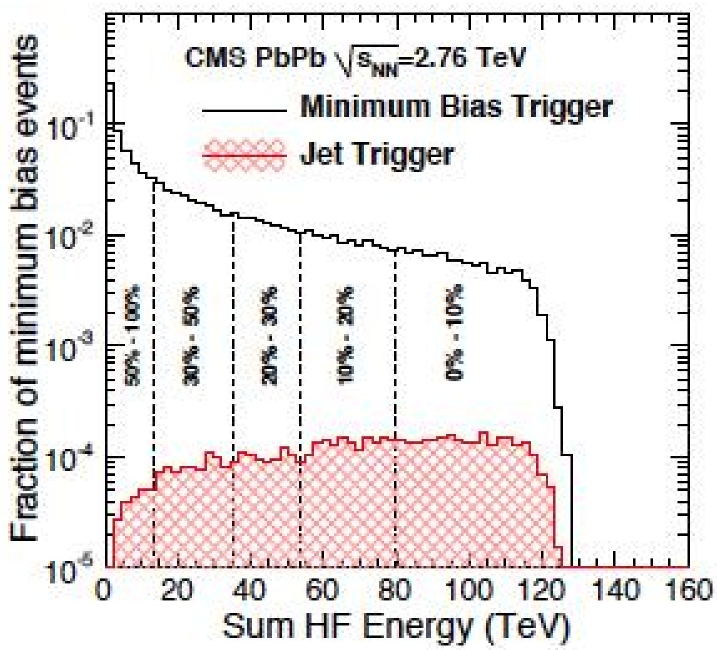

Figure 2.10. Distribution of the total HF energy for minimum bias collisions. The five regions correspond to the centrality ranges are shown. Also, HF energy distribution is shown for events passing the HLT jet trigger (red-hatched histogram).

Simulations can be used to correlate centrality, as quantified using the fraction of the total interaction cross-section, with more detailed properties of the collision. The two most commonly used physical quantities are the total number of nucleons in the two lead (^{208}Pb) nuclei which experienced at least one inelastic collision, denoted as N_{part}, and the total number of binary nucleon-nucleon collisions, N_{coll}.

The centrality bins can be correlated to the impact parameter, *b*, to average values and variances of N_{part} and N_{coll} using a calculation based on a Glauber model in which the nucleons are assumed to follow straight-line trajectories as the nuclei collide (CMS Collaboration, 2010). The bin-to-bin smearing of the results of these calculations due to the finite resolution and fluctuations in the HF energy measurement was obtained from fully simulated and reconstructed MC events generated with the AMPT event generator (Lin Z.W., Ko C. M., Li B.-A. et al, 2005). Standard parameters of the Woods-Saxon function used to model the distribution of nucleons in Pbnuclei. (Vries H. De, De Jager C.W., and Vries C. De, 1987).

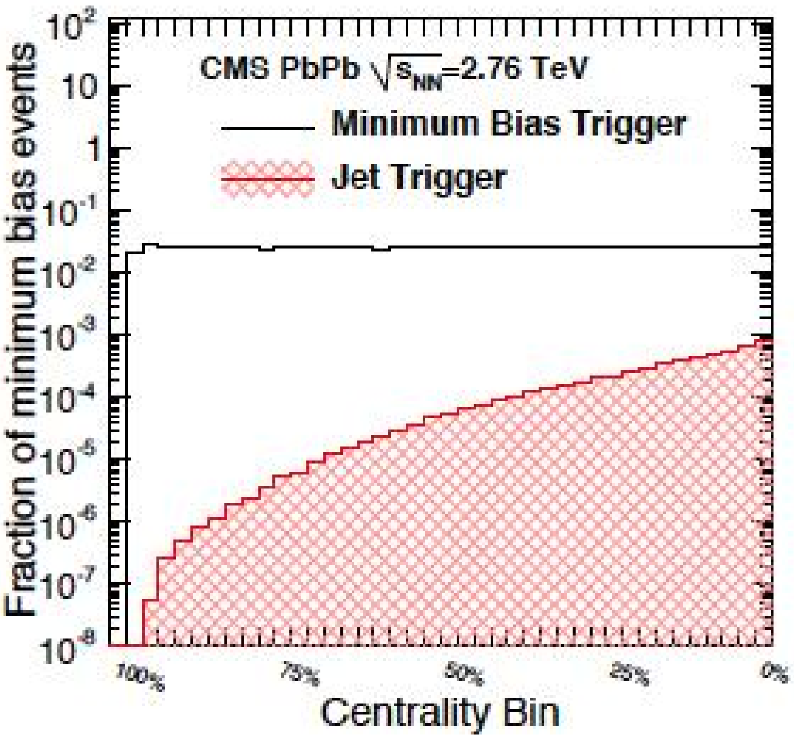

Figure 2.11. Distribution of the fraction of events in the 40-centrality bins for minimum bias triggered and HLT jet triggered (red-hatched histogram) events.

The uncertainties in the parameters involved in these calculations contribute to the systematic uncertainty in N_{part} and N_{coll} for a given bin. The other source of uncertainty in the centrality parameters comes from the determination of the event selection efficiency.

It is important to note that the selection of rare processes, such as the production of high-p_T jets, leads to a strong bias in the centrality distribution of the underlying events towards more central collisions, for which N_{coll} is very large. This can be seen in the Figure 2.10, where the HF energy distribution for events selected by the jet trigger is shown in comparison to that for minimum bias events. The bias can be seen more clearly in the Figure 2.11 at previous page, where the distribution of minimum bias and jet-triggered events in the 40-centrality bins are shown.

2.3.6. Jet Reconstruction at CMS for *Pb-Pb* Collisions

Since the occurence of the first high-energy colliders in the 1980's, the study of "jets" has proved to be a powerful tool for probing the dynamics of Quantum Chromodynamics (QCD). Jets have been comprehensively studied at e^+e^- (LEP, SLC), ep (HERA) and $\bar{p}p/pp$ (Tevatron, RHIC, LHC) colliders, with a wide variety of jet algorithms, including infrared and collinear (IRC) safe algorithms. (Cacciari M. et all, 2010)

The jets in heavy ion (HI) collisions can be used to probe the hot, dense medium. In the past few years, the Relativistic Heavy Ion Collider (RHIC) has collected significant numbers of copper-copper and gold-gold collisions at nucleon-nucleon centre of mass energies, and the Large Hadron Collider (LHC) delivered high yields of lead-lead collisions at much higher energies. The main difficulty to studying jets in HI collisions is the presence of the huge background given by the underlying event produced simultaneously with the hard nucleon-nucleon collision. This underlying events needs to be properly subtracted from the momentum of a given jet in order to find its "true" momentum and energy.

The experimental definition of a jet in nucleoncollisions is not directly derived from theory, so we need to study the different observablesat several energy ranges,so establishingan experimental definition of a jet. In addition, this definition needs to be modifiedto account for detector inefficiencies, such as, materialize in acceptancetables that determine which particles can be detected and which cannot. In heavy-ion collisions, where jets appear over a strong thermal background ofcollective motion and possibly mini jets, defining a jet and analyzing the effects ofbackground noise on the different jet observables becomes an essential and inherentlydifficult task. In this section, jet-finding algorithm is defined and mentioned step by step. For first heavy ion collisions at LHC, jets are found with iterative cone algorithm. (Kodolova O., Vardanian I., Nikitenko A. et al., 2007), (Cacciari M., Rojo J., Salam G. et al 2010).

Iterative Cone Algorithm:

1. Consider the most energetic final state particle with coordinate $(h_{\max}, f_{\max})$and set $h^{jet} = h_{\max}$ and $f^{jet} = f_{\max}$. If energy of this particle is below 1 GeV, then terminate.This is our jet seed.

2. Loop over all final state particles and determine which one is inside the jet cone; that is, determine for which particle following condition *is* satisfied $\sqrt{(h^i - h^{jet}) + (f^i - f^{jet})^2} \leq R$ where *R* is the jet radius. (2.1)

3. Use the particles inside the cone to recalculate the jet kinematic variables:

$$E_T^{jet} = \sum_{i\hat{I}jet} E_T^i \quad (2.2)$$

$$h^{jet} = \frac{1}{E_T^{jet}} \sum_{i\hat{I}jet} E_T^i h^i \quad (2.3)$$

$$j^{jet} = \frac{1}{E_T^{jet}} \sum_{i\hat{I}jet} E_T^i j^i \quad (2.4)$$

4.If $\Delta R = \sqrt{(h_{old}^{jet} - h^{jet})^2 + (f_{old}^{jet} - f^{jet})^2} \leq 0.01$ then remove the particles inside this jet from the list of particles, add this jet to the list of jets found and return to step 1. If ΔR> 0.01, then return to step 2 and iterate the algorithm using the jet coordinates found in step 3. If there is no convergence after 100 steps return to step 1.

2.4. Background Subtraction

2.4.1. Underlying Event Contribution to Heavy Ion Events

In heavy ion collision experiments at the LHC, the medium-induced energy losses of a hard partonic jet propagating through the dense matter can provide information on the quark–gluon plasma. In order to observe these losses in a jet, one should also measure the energy and direction of jets with good resolution. The main challenge in the jet recognition in heavy ion collisions is to distinguish them from the “false” jet background arising from fluctuations of the transverse energy flow from the large multiplicity of secondary particles in the event. Predictions vary from 2000 to 8000 charged particles per unit of rapidity in central *Pb–Pb* collisions at the LHC. Under these terms, the reconstruction of “true” QCD jets resulting from hard parton-parton scattering is very important. The definition of an object like a jet is difficult inPbPbcollisions. In particular, the energy and spatial resolution of jets are sensitive to the parameters of the jet finding algorithm. An original jet finding algorithm was developed for reconstructing hard jets in heavy ion collisions (Baur G. et al, 1999), (Kodolova O. et al., 1998), where particles produced in a typical collision deposit a transverse energy E_T of up to 10GeV in every calorimeter tower. The algorithm allows subtraction of the background energy due to the underlying event energy flow and identification of the hard jets on an event-by-event basis. In this study, the background subtraction algorithm studied and performed for obtaining theefficiency of pileupsubtraction algorithm.

Jet reconstruction in heavy-ion collisions in CMS is performed primarily with an iterative cone algorithm modified to subtract the underlying soft background on an event-by-event basis. Initially, the mean value and dispersion of the energies recorded in the calorimeter cells are calculated for all rings of cells at constant pseudorapidity, η. The value of this pedestal function, $P(\eta)$, containing the information on the mean and dispersion, is then subtracted from all cells. If cell energy comes out negative, then the cell energy is set to zero. The algorithm subtracts $<E_{cell}> +\sigma(E_{cell})$ from each cell in order to compensate for the bias caused by this elimination of negative energy. Jets are then reconstructed using a standard iterative cone algorithm, from the remaining non-zero cells. In a second iteration, the pedestal function is recalculated using only calorimeter cells outside the area covered by reconstructed high p_T jets (p_T> 10 GeV/c). The threshold of 10 GeV/c was chosen to optimize the final extracted jet energy resolution. The cell energies are updated with the new pedestal function (again subtracting mean plus dispersion) and the jets are reconstructed once more using the updated calorimeter cells. The detailed information about performance of Iterative Cone algorithm can be found in reference (Kodolova O., Vardanian I., Nikitenko A. et al., 2007). To understand the amount of background for a jet, a study is performed on the ***Pb-Pb*** data.

2.4.2Pileup Subtraction Algorithm to Subtract the Background

Heavy Ion jet finding algorithm has been developed to search for “jet-like” clusters above the average transverse energy flow and to subtract the background due to the underlying event.

The algorithm is a variant of an iterative “noise/pedestal subtraction” technique. Initially, the mean value of energy and mean dispersion in a cell are calculated for all ηrings, i.e. the pedestal as a function of η ($P(\eta)$) is determined. Then the value of the pedestal function ($P(\eta)$) is subtracted from all cells and jets are found from the remaining non-empty cells. After the pedestal subtraction, a cut on the transverse jet energy E^T_{cut} is applied. The value of the E^T_{cut} is defined using events without recognized jetsafter pedestal subtraction and is 30GeV for PbPb eventand 10 GeV for high-lumi pileup. After applying the cut,the value of the pedestal function is recalculated using cellsoutside the jet area.

The Pile up subtraction algorithm is described step-by-step here.

- As a first step, the average tower transverse energy $\overline{E_T^{tower}(h)}$ and its standard deviation $s_T^{tower}(h)$ are calculated event by event at each η ring over all towers in the barrel and endcap calorimeters. The standarddeviation is defined as;

$$\sigma_T^{tower}(\eta) = \sqrt{\overline{\left[E_T^{tower}(\eta)\right]^2} - \left[\overline{E_T^{tower}(\eta)}\right]^2} \tag{2.5}$$

In a next step, all tower energies are recalculated as

$$E_T^{tower*} = E_T^{tower} - \overline{E_T^{tower}(\eta)} - k\sigma_T^{tower}(\eta), \tag{2.6}$$

where E_T^{tower} is the original transverse energy in the tower. If the value of the transverse tower energy after subtraction becomes negative, it is set to zero.

– Using the corrected tower energy, jets are found with an iterative cone algorithm as mentioned in Section 2.3.6.

– Then the average tower energies and dispersions are recalculated again using only towers outside of the jets, the original tower energies are used in this calculation.

– In a next step, all tower energies are recalculated as

$$E_T^{tower*} = E_T^{tower} - \overline{E_T^{tower}(\eta)} - k\sigma_T^{tower}(\eta), \tag{2.7}$$

– If the tower energy after subtraction becomes negative, it is set to zero.

– Then the iterative cone algorithm is used again to reconstruct the final jets from the towers with the new energies.

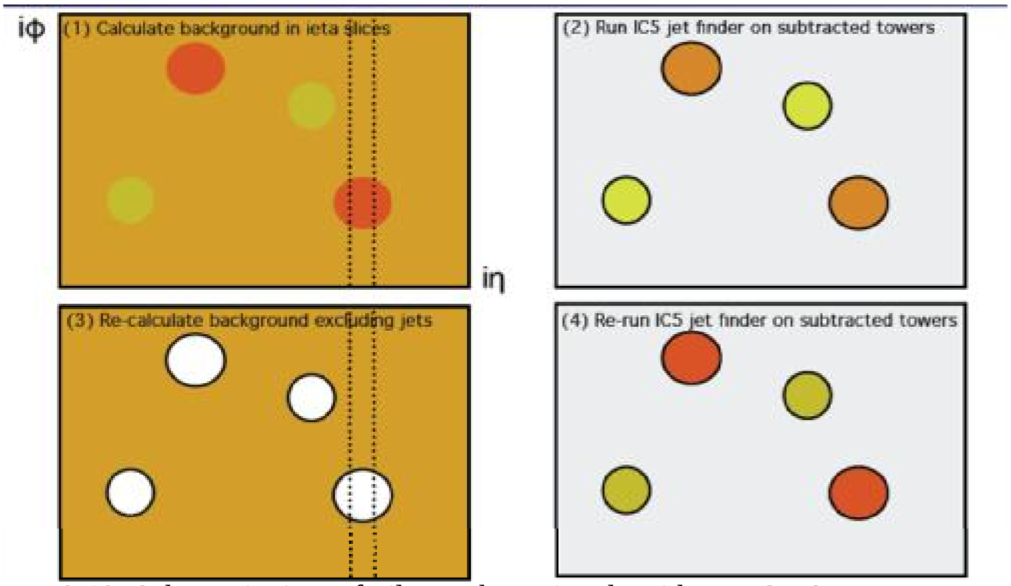

Figure 2.12. Schematicview of pileupsubtractionalgorithm at CMS

The parameter k is compensates the positive bias in the reconstructed jet energy due to zero suppression of towers with negative energies. The factor k is chosen according to the responses to the given energy flow inside the cone. The value of the parameter k will in general depend on a number of parameters, including background, jet energy and analysis cone size and type. The value k = 1 is chosen to largely eliminate the dependence of the reconstructed jet energy and energy resolution on event multiplicity in CMSPbPb collisions.

Different methods of background subtraction can be considered to reduce the effects of background events on the jet reconstruction. In all these methods, the average tower energy offset due to background (pileup, noise) contribution is evaluated event by event as a function of the tower pseudorapidity,η.

2.4.3.Random Cone Technique to Estimate the Background

The random cone technique starts with minimum bias data events for which the jets have been reconstructed and the mean and sigma of signals for ηslices of the underlying event have been determined by excluding the found jets, following the standard procedure. After this, five random points which distributed uniformly in both $\eta$and f were selected. For each point a cone of radius R = 0.5 was placed and the total energy minus the background inside this cone was determined. The distributions of the resulting background-subtracted energies should have a mean of zero but also provides an estimation of the spread of possible energies of fake jets resulting from fluctuations in the underlying event.

2.4.4. Estimation of Background with Embedding Signal Jet to Real Data

In order to study the effect of the large underlying events present in PbPb collisions on the reconstruction of jets, simulated jets with known energy were embedded into real collision data. This offers the possibility to study the impact of background subtraction on the embedded jet using the most realistic possible environment. The procedure involves pre-processing the RAW events, saving the reconstructed vertex position. For each event, which satisfiesthe minimum bias trigger and offline collision event selection, jetsare generated using PYTHIA. The origin for the particles from this jet is placed at the reconstructed vertex of the data event. The detector response to this jet is then simulated and digitized. Finally, the sample of data+jet mixed events is reconstructed in an analogous way to a normal event.

The output of this embedding procedure forms the basis of the predictions for jet properties in the absence of any medium induced modifications. Modifications to the standard procedure have been analysed to look for systematic effects. One very important result of analysing the embedded sample is the extraction of the jet energy scale and resolution. Comparing the energy found using the jet algorithm to that at the Generator level does this.

One can further evaluate the embedded events to separate different contributions affecting the jet energy resolution. Although the pileup subtraction algorithm succeeds to subtract the background energies correctly on average, at the event-by-event level it may under or over estimate the background, causing inaccuracy in the amount of the jet energy. If one compares the reconstructed energy of the mixed event to the reconstructed energy of the MC signal, the difference would point to effects solely coming from large underlying event fluctuations and deficiencies of the pile up subtraction algorithm, which are the effects that are not present inpp collisions. The effect of fluctuations is not only the extra energy in the jet cone, but also misdetermination of the correction factor.

The embedded jets allows the ability to compare the p_T of jets reconstructed from the pure signal event to the p_T of jets reconstructed on top of a data PbPb background.

4. CONCLUSIONS

The CMS heavy ion collisions have been performed since 2010 November. At this thesis one of the first results of lead-to-lead collisions (2010 data) was showed and studied. Collisions of Pb nuclei have been never probed before the LHC. Previously at the RHIC gold nuclei were collided and results is presented at the reference (STAR Collaboration, 2009).

In this thesis the CMS jet algorithm, background subtraction method and jet properties of heavy ion collisions were studied. The study showed that background subtraction algorithm works very well. But in some cases the background was subtracted much or less then it should. It is shown that the fluctuation of the background is Gaussian and has positive and negative tail.

Also, in this thesis shown that, the collision centrality determination is performed on HF calorimeter hits. But on the other hand the barrel energy region can be used for determination of the centrality. In this study, the centrality is determined and compared using both HF and barrel energy deposition.

3. RESEARCH AND DISCUSSIONS

3.1. Tower Energy Spectrum

The PbPb collision has not performed before anywhere in the world . Due to this fact there was no trustable Monte Carlo simulations to explain this collisions. But after the first collisions at the LHC, we observed that our MC simulation was highly consistent with real PbPb collisions. The study will rely on the comparison of heavy ion collision data with MC simulations. MC simulation is performed by HYDJET and AMPT simulators.

The towers which are software objects that combine information from ECAL and HCAL calorimeter are used in the calorimeter-based jet reconstruction. The towers are called as CaloTowers, which means calorimeter towers. The η - ϕ segmentation of towers are defined by the HCAL tower boundaries. All calorimeter cells contained in the respective $\eta - \phi$ region are associated as tower and considered its constituents. The reconstruction of a tower includes 25 ECAL crystals and 1 HCAL crystal at different depths. Deposited energy via incident particles in each crystal is accumulated to form one tower energy.

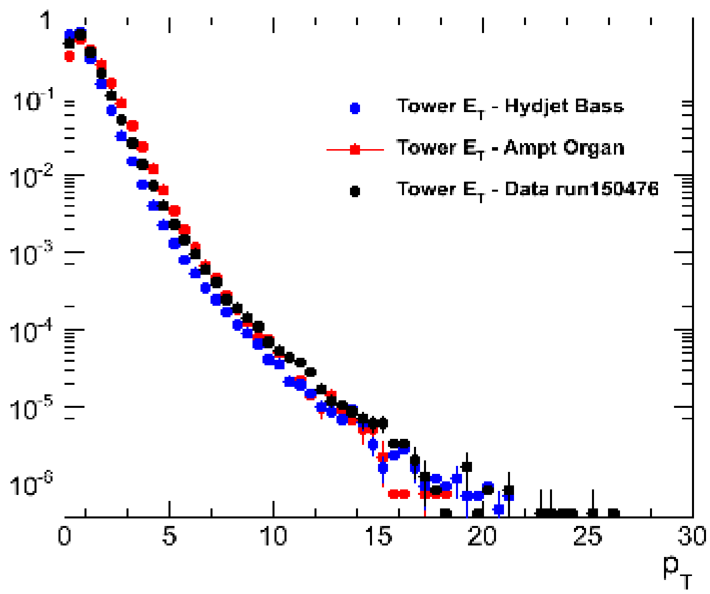

Figure 3.1. The tower transverse momentum spectrum of CMS heavy ion collision data with MC.

Comparison of the tower energy reconstructed at CMS and predicted by MC simulation is shown at Figure 3.1. As can be seen from the figure the real data and predicted simulation is highly matched and consistent. The comparison is performed at mid rapidity region (|η| < 1) for all centralities.

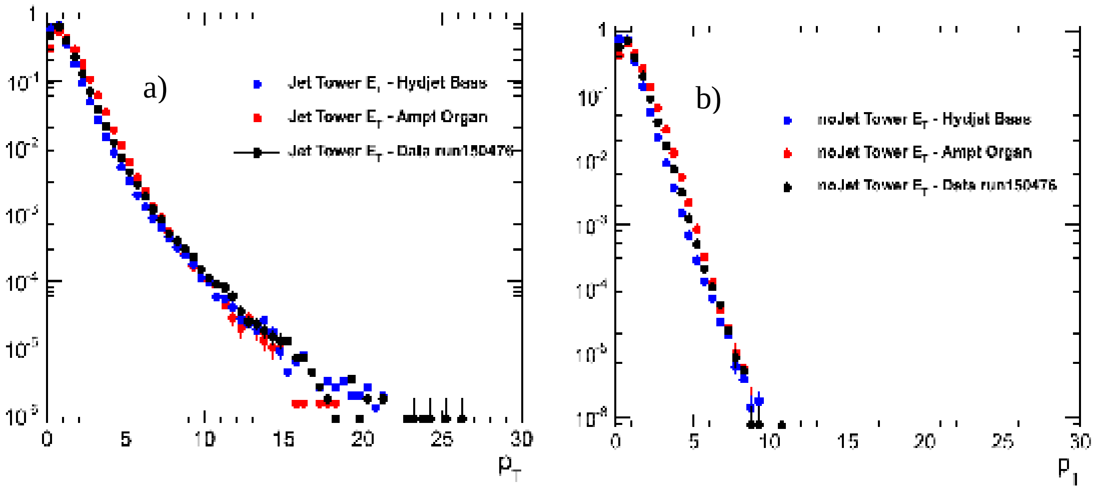

Figure 3.2. The tower transverse momentum spectrum inside (left) and outside (right) of the jet cone. The Comparison is based on first CMS heavy ion data and MC (HYDJET and AMPT).

The jet associated tower transverse momentum spectrum can be seen in Figure 3.2(a). The tower transverse momentum of outside of the jet cones can be seen in Figure 3.2(b).

3.2. Jet Energy Spectrum

The Calorimeter jets also called CaloJets are expected to yield a good description of both the parton-level and the hadron showers emerging from the hard interaction. For Monte Carlo events, the hadron-level is defined by applying the same clustering algorithms, which are typically formulated to accept any set of four vectors as inputs, to all stable particles from the MC truth record called as GenJets. Hadron-level is also referred as “particle-level”.

Calorimeter jets are reconstructed using energy deposits in calorimeter towers (CaloTowers) as inputs: they are composed of one or more HCAL cells and corresponding ECAL crystals. The rough sum of energy deposits of one single HCAL cell and 5x5 ECAL crystals form a projective tower in the barrel ($|\eta| < 1$). The standard jet reconstruction applies the "Scheme B" thresholds on calorimeter cells. The reconstruction algorithm is examining the all CaloTowers and eliminating the towers below the thresholds (see Table 3.1.). Then reconstruct the jets as a calorimeter jets.

Table 3.1. Calotower Thresholds (Scheme B).

Threshold Name	GeV
HB Threshold	0,9
HO Threshold	1,1
HES Threshold	1,4
HED Threshold	1,4
EBSum Threshold	0,2
EESum Threshold	0,45

Subject to predefined thresholds, the energy of ECAL and HCAL RecHit energies are each summed together to get the electromagnetic and hadronic energy in a CaloTower. In the barrel region, the HCAL contributions from HB and HO are saved separately. If the summed electromagnetic or hadronic energy is below a predefined value, the corresponding contribution to the tower energy is set to zero. The thresholds act as two levels of filtering of low energy contributions: at RecHit and CaloTower level. The thresholds themselves are defined in a configuration file controlling CaloTower reconstruction.

3.3. Event by Event Mean and Standard Deviation of Tower Energy

As mentioned in *Section* 2.4.2. the pileup subtraction algorithm is performed by event-by-event basis on subtracting the mean+standard deviation of tower energies outside the jet cone. Mean and standard deviation of tower energies were determined for each eta slice in barrel region(|η|<1) but outside jet cone. Mean+standard deviation is filled to histogram. The histogram was fitted with Gaussian and results are shown in Figure 3.3. Mean of Gaussian gives idea about which value should be subtracted as a background from each tower energy. The mean plus standard deviation of each tower corresponds to the 1,3, 1,14 and 1,2 GeV for HYDJET, AMPT and Hydro simulation data respectively as can be seen from Figure 3.3. Mean plus standard deviation of tower energies are fluctuating around 1 GeV for three different simulation data(see the same figure). Then pileup algorithm should subtract ~1 GeV from each tower energy. This figure just gives a idea of pile subtraction method for heavy ion collisions.

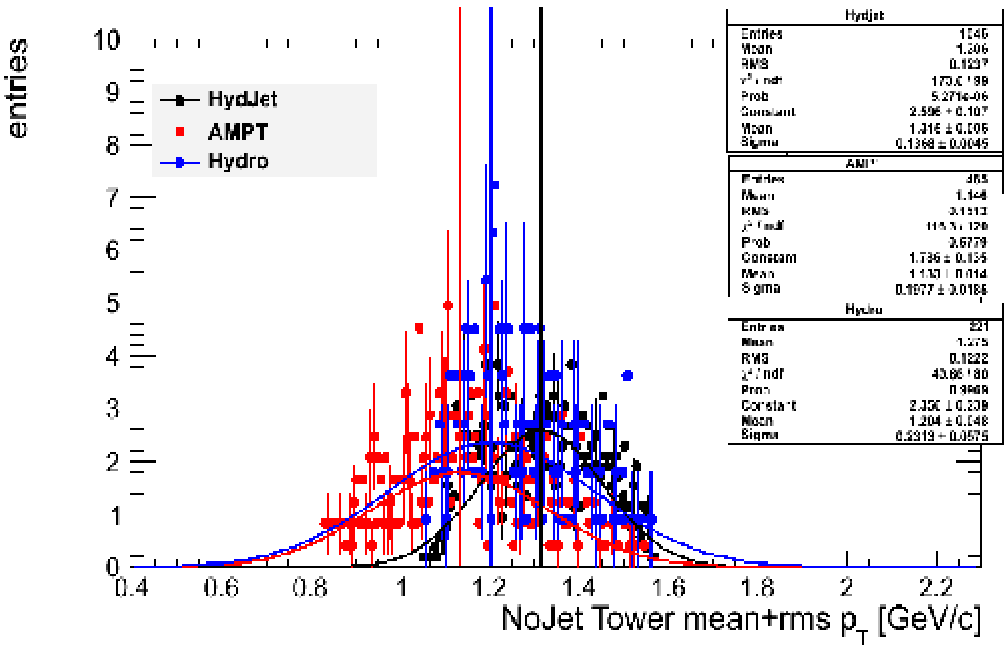

Figure 3.3. The mean plus standard deviation of tower energies for different MC

3.4 Estimation of Cone Energy with Toy MC

Estimation of cone energy with toy MC method is based on converging two probabilities. First probability is tower energy spectrum and second one is probability of number of tower inside the jet cone. One can choose randomly a jet cone with known number of towers and give energy to all of the towers from tower energy spectrum, so that, can estimate the energy of the jet cone. In fact the jet area and the tower area is constant.

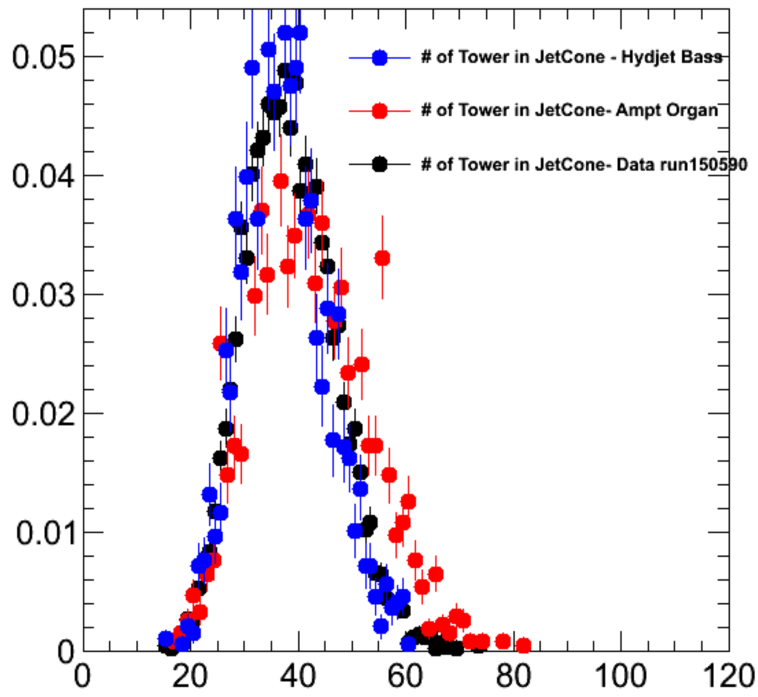

Figure 3.4. The number of jet associated towers

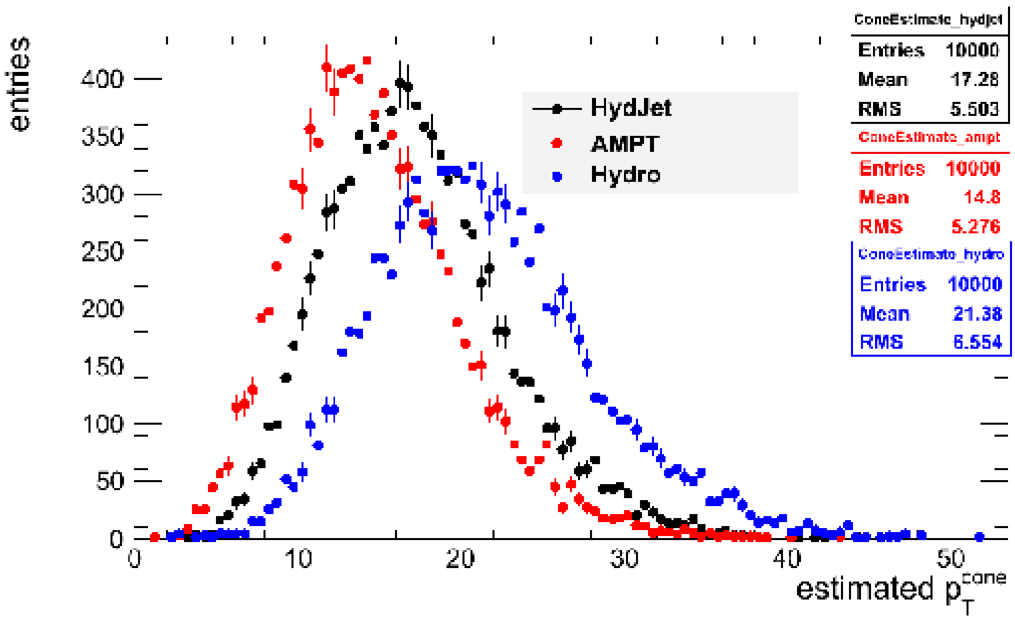

Figure 3.5. Estimated cone energy with Toy MC method for different MC models.

Since the tower area is $0,087\eta\times0,087\phi$ and the number of towers inside a jet cone with a radius 0,5 is around 100(jet area/tower area). But because of the zero suppression(towers without hit), the number of towers inside the jet cone is not constant since number of towers without hits changes randomly. This calculation is called as Toy MC method because it is easy. In Figure 3.4, the jet associated tower numbers is shown. As can be seen from the plot, number of towers associated to jet cone is averagely 40 for MC and real data. Consistency of HYDJET simulation data with real data is pretty better then AMPT simulation data. After the selection of tower number inside the jet cone from Figure 3.4 and tower energies spectrum from the Figure 3.1 we can estimate the jet cone energy with toy MC method. Figure 3.5 shows the estimated cone energy inside the jet cone with random detector phase space. Estimated energy of jet cone is calculated as about 20 GeV, 15 GeV, 17 GeV for Hydro, AMPT and HYDJET simulation data respectively.

3.5. Random Cone Energy Without Pileup Subtraction

An other approach to estimate the background contribution to a jet cone energy is performed by placing the virtual jet cones inside the calorimeter randomly. This method is called as random cone technique and explained in Section 2.4.3. Figure 3.6 shows the energy of randomly selected jet cone inside the calorimeter without any background subtraction. As can be seen from the Figure 3.6 measured cone energy without background subtraction is about 70 GeV. This result is far from the our Toy MC calculations (20 GeV). The random cone technique provide more realistic estimation of cone energy comparing to toy MC technique.

The random cone energy without background subtraction is shown in Figure 3.6. It is expected to be same with Figure 3.7. But as can be seen from the Figure 3.6 and Figure 3.7 they don’t have the same energy distribution. The centrality parameter of heavy ion collisions is determined by HF energy deposits and same method used for Figure 3.7. But for Figure 3.6. event selection were done using deposited energy in barrel region.

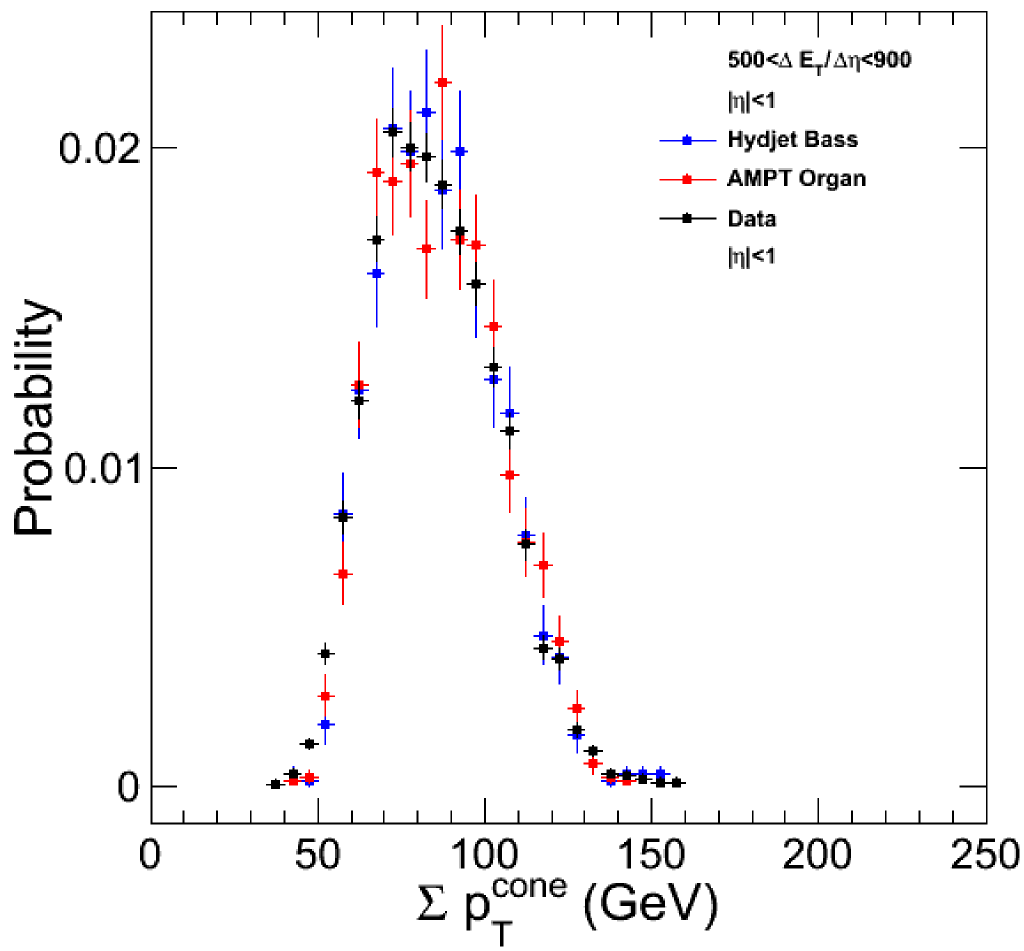

Figure 3.6. Random Cone Energy without background subtraction for real data and MC (HYDJET and AMPT). Event Selection based on total energy of barrel calorimeter region (500 GeV $<\Delta E_t / \Delta\eta < 900$ GeV and $|\eta|<1$).

When centrality selection is switched to HF calorimeter energy deposits, the agreement is worse then using energy deposited in barrel region. Figure 3.7 shows that, AMPT simulation is simulate the cone energy more than data, but HYDJET simulation still has good agreement with data. Measured cone energy with HF selection, is about 100 GeV for real data, is ~80 GeV for HYDJET and is ~130 GeV for AMPT simulation.

3.6. Random Cone Energy After Background Subtraction

Random cone technique provide the virtual jet cones which are acting like real jet. This virtual jets has energy, momentum, coordinates, jet axis, background, etc. After placing random cones in the detector virtually, all algorithms can work on the virtual jets for obtaining the properties of them as real jet.

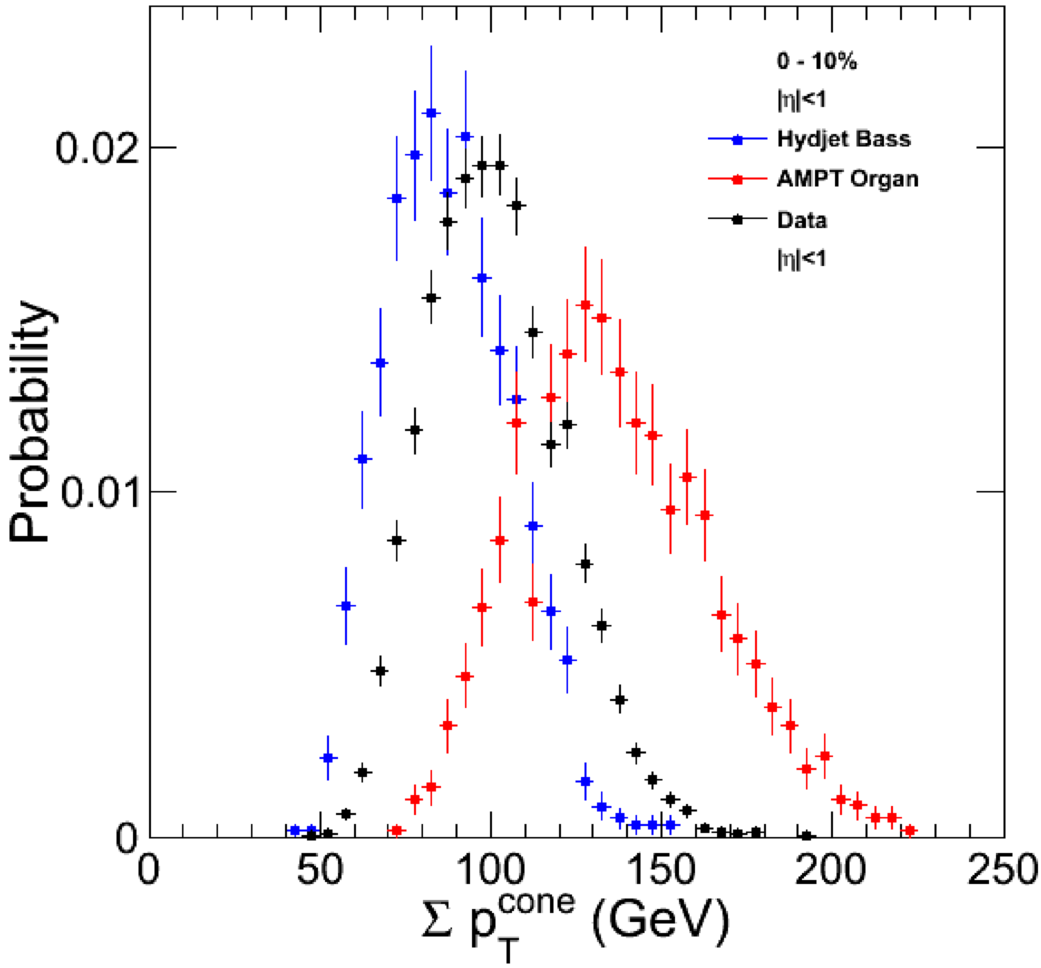

Figure 3.7. Random Cone Energy for data and MC. Event selection performed by energy deposit in HF calorimeter. (Most central events and |η|<1).

For instance, background calculation of the this virtual jets are determined by pileup subtraction algorithm. Pileup Subtraction algorithm determines the background contribution to jet cones and subtract the unwanted contributions from the jet energies. For random jet cones the background contributions are determined by pileup subtraction algorithm and removed from the cone energies same as the real jets. The result is shown in Figure 3.8.

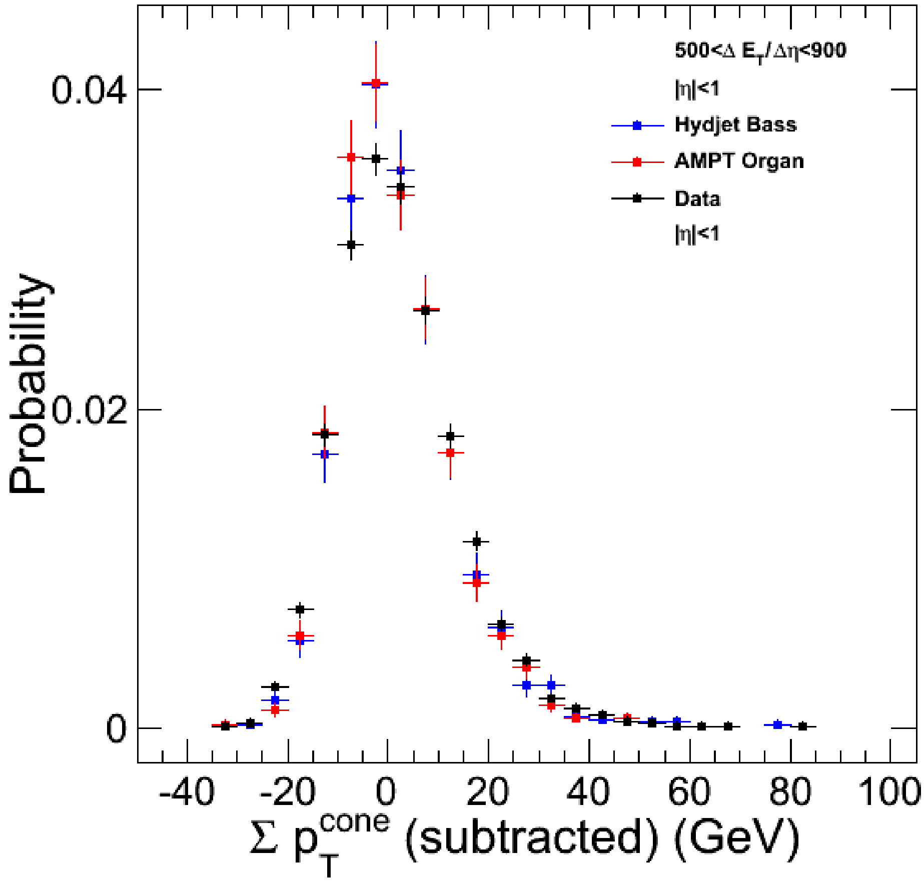

Figure 3.8. Background subtracted random cone energy. Event selection based on total energy in the barrel calorimeter (500 GeV $<\Delta E_t$ / $\Delta\eta$ < 900 GeV and $|\eta|<1$).

If one remove the background contribution from the real jets, there would remain the real jet energy which must greater than zero. But if one remove the background contribution from the random jet cone, there would remain no energy! Because of random cones placed in detector randomly, the energy of random cones would just comes from the background contribution since they do not contain any component of real jet (parton scattering etc.). So we can call them like background jets. If background contribution is removed properly from the random cones there wouldn't remain any energy inside the random cone. Because of this reasons, background subtracted cone energy peaks at zero as can be seen in Figure 3.8. But, background subtracted cone energy also have valuable negative and positive tails. These Gaussian distribution is telling that, pileup subtraction algorithm is mostly subtracting background well. But sometimes algorithm subtracting too much or too less. This is result of background fluctuations. Background are not homogenously distributed in the calorimeters. It does not has uniform shape and does fluctuating inside the calorimeters. Background fluctuations is characterized by underlying events.

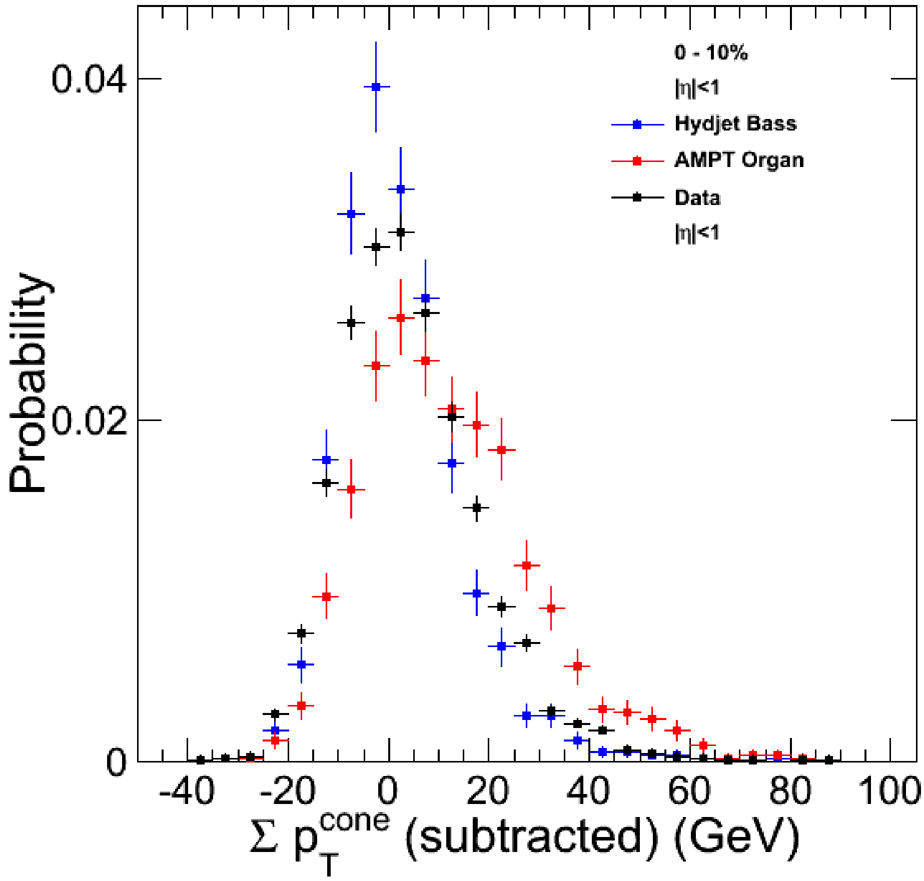

Figure 3.9. Background subtracted random cone energy for data and MC. Event selection performed by energy deposit in HF calorimeter. (Most central events and |η|<1)

Background subtracted random cone energies peak at zero and has Gaussian distribution as can be seen in Figure 3.9. Event selection is done using energy deposit in HF calorimeter for Figure 3.9. Figure 3.8 and Figure 3.9 show the same result. But because of different event selection, real data and MC consistency is different. As can be seen from Figure 3.8 and Figure 3.9, real data and MC is more consistent when barrel calorimeter energy deposit is used for event selection.

As a result, random cone energies after the background subtraction is mostly around zero. After the background subtraction background inside the jet cones wouldn't remain too much. So the jet energies can be measured with great accuracy.

3.7. Comparison of Two Methods Random Cone and Embedding Technique

Instead of random cone technique one can use the Embedding technique which is explained in the section 2.4.4. After embedding the signal jets to the real background data, the signal jet tower energies is removed from the jet cone and remaining energy inside the cone is measured.

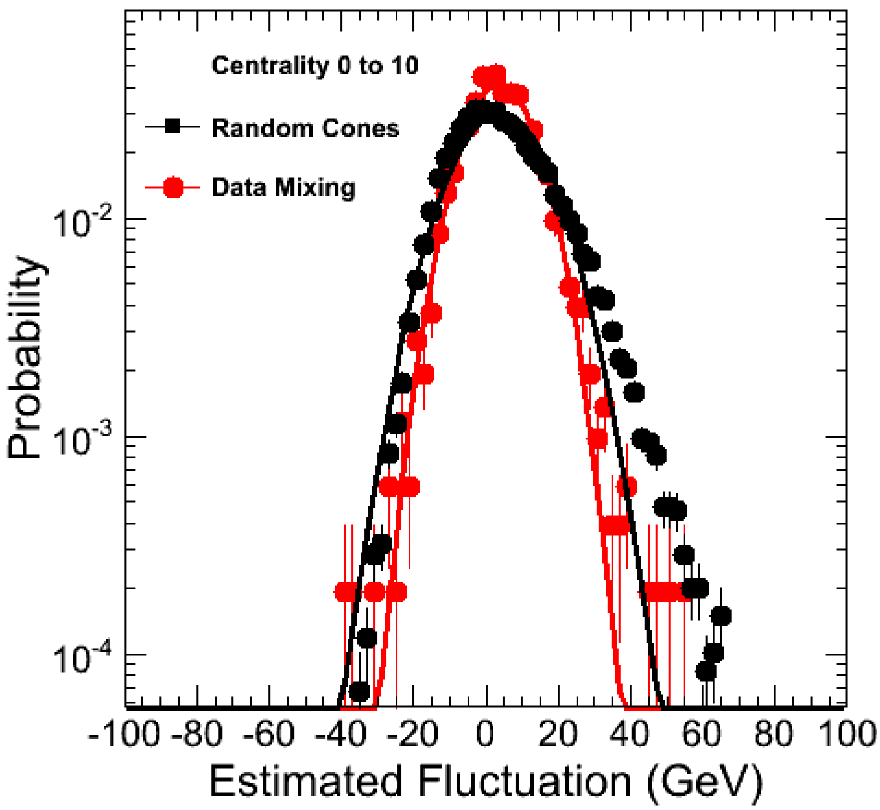

Figure 3.10. The comparison of embedding technique and random cone technique for centrality of %0 to %10.

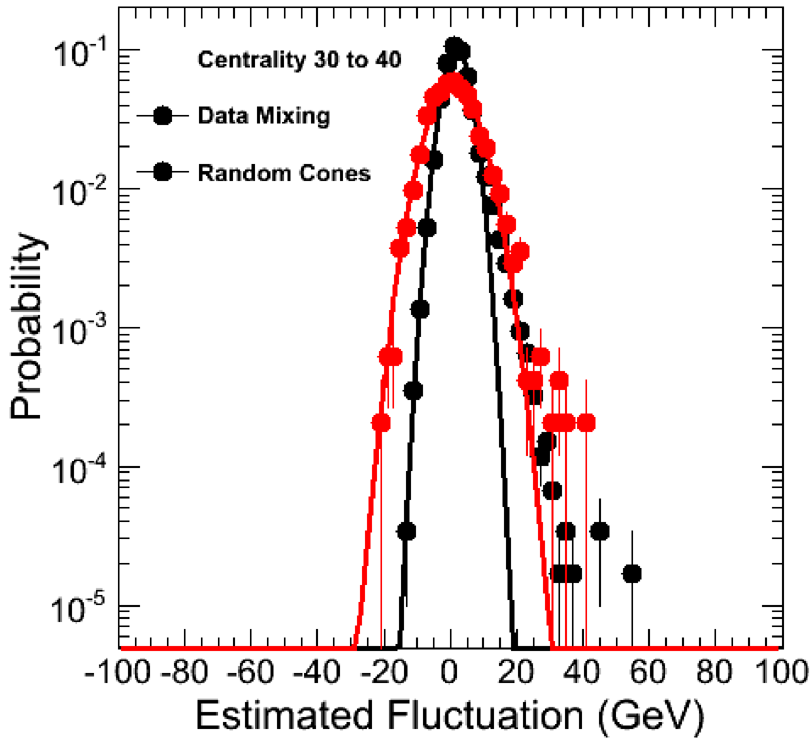

Figure 3.11. The comparison of embedding technique and random cone technique for centrality of %30 to %40.

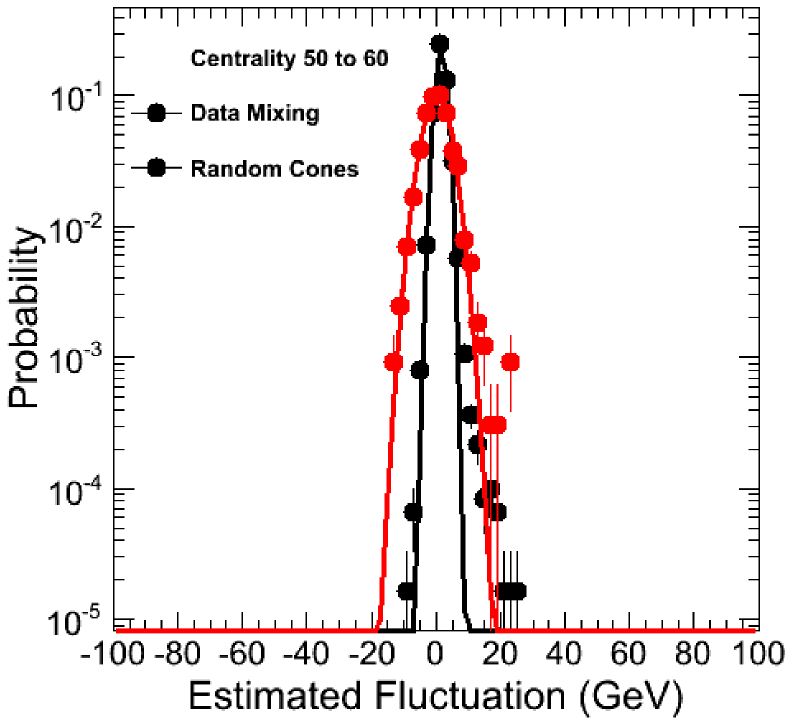

Figure 3.12. The comparison of embedding technique and random cone technique for centrality of %50 to %60.

Random cone and embedding tecniques compared and results are shown in the Figure 3.10, Figure 3.11 and Figure 3.12. The black dots are pointing the random cones and red dots are embedded cones. Figure 3.10 is obtained for most central events (%0-%10 central). Figure 3.11 is obtained for semi-central events (%30 - %40). Figure 3.12 is obtained for peripheral events (%50-%60).

As seen from the Figure 3.10 the embedding technique gives Gaussian shape curve within +40 GeV and -40 GeV energy range. But random cone technique gives different results at the positive tail side. Positive tail might come from the overlap of real jet and random cone. Random cones placed in detector randomly and it might overlap with some part of real jets. When this overlapping happens, random cone energy would be more than the background and greater than zero after background subtraction.

For most central events, remaining cone energies is higher than the semi-central and peripheral events.

As can be seen from the plots, data mixing and random cone technique is quite similar. As a result of two techniques the amount of background energy remained inside the jet cone after pile up subtraction is mostly peak at zero. And plots are showing that pile up subtraction algorithm is working well.

3.7. Efficiency of Pileup Subtraction Algorithm

Efficiency of pileup subtraction algorithm was explained in previous sections. As can be seen from the Figure 3.8 and Figure 3.9, after the pileup subtraction the peak is at the zero for both. It means that: pileup subtraction algorithm is mostly subtracting the background from jet cone properly. On the other hand, we have the tail on the right and left side of Gaussian curve in Figure 3.8 and Figure 3.9. The positive side of the Gaussian curve means that the pileup subtractor is removed background less and while negative side means more than expected.

On the real jet side, if pileup subtractor is remove too much energy from the jet cone as a background, some part of real jet energy will be lost. Similarly, if pileup subtractor remove less background from the jet cone, jet energy will be unreliable.

According to random cone and embedding techniques, background subtraction from the jet cones working properly. In less cases, background subtracted much or less, Anyhow in most cases, background is removed from jet cones properly which means efficiency of pile up subtraction algorithm is good.

REFERENCES

BAUR G. ET AL., CERN CMS NOTE 1999/016

CACCIARI M., ROJO J., SALAM G. ET AL., 2010. “Jet Reconstruction in Heavy Ion Collisions”.

CACCIARI M., SALAM G., AND SOYEZ G. , 2011. “Fluctuations and asymmetric jet events in PbPbcollisions at the LHC”

CMS COLLABORATION, 2010. “Electromagnetic calorimeter commissioning and performance with 7 TeV data”, CMS Note 10-002

CMS COLLABORATION, 2007 “High Density QCD with H e a v y Ions Physics Technical DesignReport”

CMS COLLABORATION, 2010 “Identification and Filtering of Uncharacteristic Noise in the CMS Hadron Calorimeter”, JINST 5 T03014

CMS COLLABORATION, 2010 “Observation and studies of jet quenching in PbPb collisions at sNN = 2.76 TeV” arXiv:1102.1957,

KODOLOVA O. ET AL., CERN CMS NOTE 1998/063

KODOLOVA O., VARDANIAN I., NIKITENKO A. ET AL., 2007 “The performance of the jet identification and reconstruction in heavy ions collisions with CMS detector”, Eur. Phys. J. C50 117.

LIN Z.-W., KO C. M., LI B.-A. ET AL. 2005 “A multi-phase transport model for relativistic heavy ion collisions”, Phys. Rev. **C72** 064901

MILLER M. L., REYGERS K., SANDERS S. J.ET AL. 2007 “Glauber modeling in high energy nuclearcollisions”, Ann. Rev. Nucl. Part. Sci. **57** 205

OWENS J. F. , 1987. *Rev. Mod. Phys.,Vol.* 59, No. 2, 465

PHENIX COLLABORATION, S. S. ADLER ET AL., 2005 “Systematic studies of the centrality and *!sNN* dependence of dE(T)/deta and d N(ch)/deta in heavy ion collisions at mid-rapidity,” *Phys. Rev.* **C71** 034908

SAHOO R., CHATTOPADHAYA S., SUAIDE A. A. P., DE MOURA M. M., AND MAHAPATRA D. P., 2006 “Transverse energy measurement in *!sNN* = 62.4 GeV Au + Au collisions at RHIC,” *Rom. Rep. Phys.* **58** 055–062

STAR COLLABORATION, 2009 “First Direct Measurement of Jets in sNN = 200 GeV Heavy IonCollisions by STAR”, Eur. Phys. J. **C61** 761

STAR COLLABORATION, 2009 “First fragmentation function measurements from full jetreconstruction in heavy-ion collisions at psNN = 200 GeV by STAR”, Eur. Phys. J. **C61** 629,

STAR COLLABORATION, 2009. “Inclusive cross section and correlations of fully reconstructed jets in 200 GeV Au+Au and p+p collisions”, Nucl. Phys. **A830** 255C

STAR COLLABORATION, 2009 “Measurements of jet structure and fragmentation from full jetreconstruction in heavy ion collisions at RHIC”, Nucl. Phys. **A830** 267C

WIEDEMANN U. A *ET AL.*, 2003 "Hard Probes in Heavy Ion Collisions at the LHC: Jet Physics", hep-ph/0310274,

VRIES H. DE, DE JAGER C.W., AND VRIES C. DE, 1987 “Nuclear charge and magnetization density distribution parameters from elastic electron scattering”, Atom. Data Nucl. Data Tabl. **36** 495.

CURRICULUM VITAE

I was born in 1985, in Adana. I completed my primary school education in Orhangazi Elementary School and secondary school education in İstiklal Middle School. After that, I enrolled to Turgut Özal high school. I graduated from the Physics Department of Çukurova University in 2007. I have started my MSc degree at the Physics Department of Çukurova University in 2007. For my researches I spend one of my year in CERN at Switzerland with heavy ion group.